Series: **PHYSICS and ASTRONOMY**

Solomon I. Khmelnik

Hexagonal storm on Saturn

Content

1. Introduction
2. Summary of mathematical model of water vortex on the Earth
3. Mathematical model of elliptic vortex
4. Mathematical model of hexagonal vortex
Appendix 1. Solution of Maxwell's equations in cylindrical coordinates
Appendix 2. Decomposition of hexagon into ellipses.
References

Abstract

At the north pole of Saturn has more than 30 years there is a giant storm in the shape of a hexagon, each side of which is greater than the diameter of Earth. This hexagon does not move on the planet, rotates and maintains its shape. This phenomenon still has no explanation. The following is a mathematical model of such a storm similar to the mathematical model of an ocean whirlpool (proposed earlier by the author). Also in the article shows that the energy source, that allows the storm to spin for a long time, is the gravitational field of Saturn.

1. Introduction

For more than 30 years at the north pole of Saturn, there has been a huge storm of hexagon shape, which side exceeds the Earth's diameter [1, 2]. This hexagon does not travel around the planet, but rotates keeping its shape. Existing for more than 30 years, the storm demonstrates an amazing stability. Many works is dedicated to building mathematical models of this storm, but there has not been a generally recognized model yet [3].

The external similarity between this storm and the oceanic whirlpool is clearly noticeable — see Fig.1 and Fig.2. The main difference consists in the shapes of surfaces. We can say, emphasizing this similarity,

that on Saturn a hexagonal "gas vortex" exists unlike round water vortexes in oceans of the Earth.

Let's also notice that hexagonal gas vortexes can be observed on the Earth as well: analysis of the photos made by space satellites showed the presence of hexagonal clouds over the anomalous zone in the Atlantic Ocean known as the Bermuda Triangle - see Fig. 3 [4].

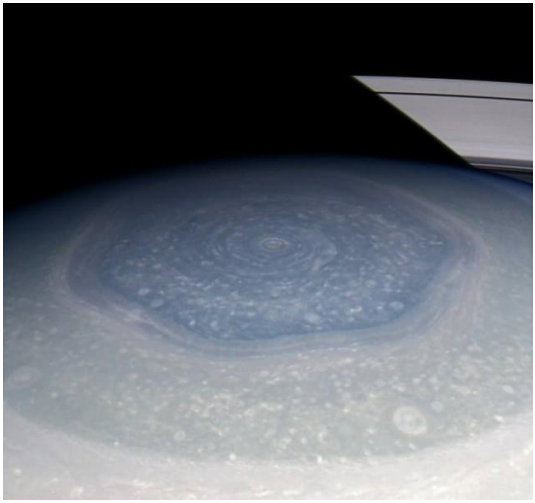

Fig. 1.

Fig. 2.

Fig. 3.

Further on, we're going to build a mathematical model of elliptic vortex first. It can be built in the same way as the round vortex model [5] based on the solution of Maxwell's equations for gravitomagnetism [6].

Then, we will show that hexagonal gas vortex is a sum of elliptic gas vortexes. Each gas vortex is determined by its own initial conditions in Maxwell's equations. In case of several sets of independent initial conditions, several solutions, or elliptic vortexes, occur. As the system of Maxwell's equations is linear, then actual solution is a sum of these solutions. The sum has a form of a hexagonal vortex.

2. Summary of mathematical model of water vortex on the Earth

In the mathematical model of water vortex [5] a system of quasi-Maxwell's gravitation equations is used [6]. The model is based on the following assumptions: Water flows can be described as mass currents. Mass currents in the gravitational field are described by Maxwell's equations for gravitomagnetism — quasi-Maxwell's gravitation equations [6] (hereinafter - QMG-equations). Interaction between moving masses is described by gravitational Lorentz forces (hereinafter — GL-forces), which are similar to Lorentz forces between moving electric charges in classical electrodynamics.

Mass currents in the vortex circulate within horizontal sections of the vortex, as well as vertically. Kinetic energy is spent on losses due to viscous friction. These energy comes from a gravitating body — the Earth. Potential energy of the vortex does not change, and therefore is

not spent, i.e. in this case, there is no conversion of kinetic energy into potential energy and vice versa. However, the gravitating body expends its energy on creating and maintaining massive currents, i.e. preserving the vortex.

The water vortex, being a type of water flow also satisfies Navier–Stokes equation for viscous incompressible liquid. In [5] it's shown that water pressure in the vortex can be calculated according to Navier–Stokes equation depending on mass currents. In this case, the locus, where vertical pressure component is constant on free surface, occurs to be a circle of given radius. Pressure at the free surface reflects the shape of the vortex surface. Therefore, the vortex surface shall contain concentric projections and deeps corresponding to wavelike dependency of pressure on radius. Based on this in work [5] an image of the vortex surface is reproduced – see Fig. 4.

The similar approach is used below. We only need to prove the existence of a solution of Maxwell's equations for elliptic vortex, and then, for hexagonal vortex.

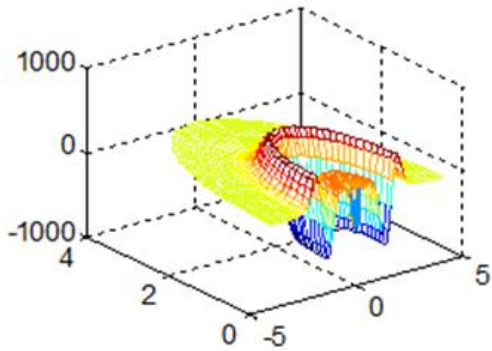

Fig. 4.

3. Mathematical model of elliptic vortex

Maxwell's equations for stationary gravitomagnetic field will be as follows:

$$\mathrm{div}(H) = 0, \quad (1)$$

$$\mathrm{div}(J) = 0, \quad (2)$$

$$\mathrm{rot(H)} = J, \quad (3)$$

where H - gravitomagnetic intensities, J - densities of mass currents.

Let's consider these equations in elliptic coordinate system ξ, φ, z [7, p. 161] - see also Fig. 5:

$$\mathrm{div}(H)=\begin{pmatrix}\frac{1}{a\Delta^3}\left(\mathrm{sh}(\xi)\mathrm{ch}(\xi)H_\xi+\sin(\varphi)\cos(\varphi)H_\varphi\right)+\\ \frac{1}{a\Delta}\left(\frac{\partial H_\xi}{\partial\xi}+\frac{\partial H_\varphi}{\partial\varphi}\right)+\frac{\partial H_z}{\partial z}\end{pmatrix}=0\,, \qquad (4)$$

$$\mathrm{rot}_\xi(H)=\left(\frac{1}{a\Delta}\frac{\partial H_z}{\partial\varphi}-\frac{\partial H_\varphi}{\partial z}\right)=J_\xi\,, \qquad (5)$$

$$\mathrm{rot}_\varphi(H)=\left(\frac{\partial H_\xi}{\partial z}-\frac{1}{a\Delta}\frac{\partial H_z}{\partial\xi}\right)=J_\varphi\,, \qquad (6)$$

$$\mathrm{rot}_z(H)=\begin{pmatrix}\frac{1}{a\Delta^3}\left(\mathrm{ch}(\xi)\mathrm{sh}(\xi)H_\varphi-\cos(\varphi)\sin(\varphi)H_\xi\right)+\\ \frac{1}{a\Delta}\left(\frac{\partial H_\varphi}{\partial\xi}-\frac{\partial H_\xi}{\partial\varphi}\right)\end{pmatrix}=J_z\,, \qquad (7)$$

$$\mathrm{div}(J)=\begin{pmatrix}\frac{1}{a\Delta^3}\left(\mathrm{sh}(\xi)\mathrm{ch}(\xi)J_\xi+\sin(\varphi)\cos(\varphi)J_\varphi\right)+\\ \frac{1}{a\Delta}\left(\frac{\partial J_\xi}{\partial\xi}+\frac{\partial J_\varphi}{\partial\varphi}\right)+\frac{\partial J_z}{\partial z}\end{pmatrix}=0\,, \qquad (7a)$$

where

$$\Delta=\sqrt{\left(\mathrm{ch}^2(\xi)-\cos^2(\varphi)\right)}\,, \qquad (7b)$$

a - half-focal distance,

coordinates ξ, φ, z correlate with orthogonal coordinates x, y, z through the following formulas

$$x=a\mathrm{ch}(\xi)\cos(\varphi),\ \ y=a\mathrm{sh}(\xi)\sin(\varphi),\ \ z=z. \qquad (7c)$$

With fixed ξ, z the point draws an ellipse in horizontal plane. With fixed φ, z the point draws a hyperbola in horizontal plane. Particularly, Fig. 5 shows ellipses and hyperbolas drawn in accordance with (7c) under $a=1$ in relation to $0\le\xi<1.2,\ 0\le\varphi<2\pi$. Fig. 6a demonstrates the same diagrams in logarithmic scale.

One of possible solutions of equations (4-7a) have the following form (as shown in Appendix 1):

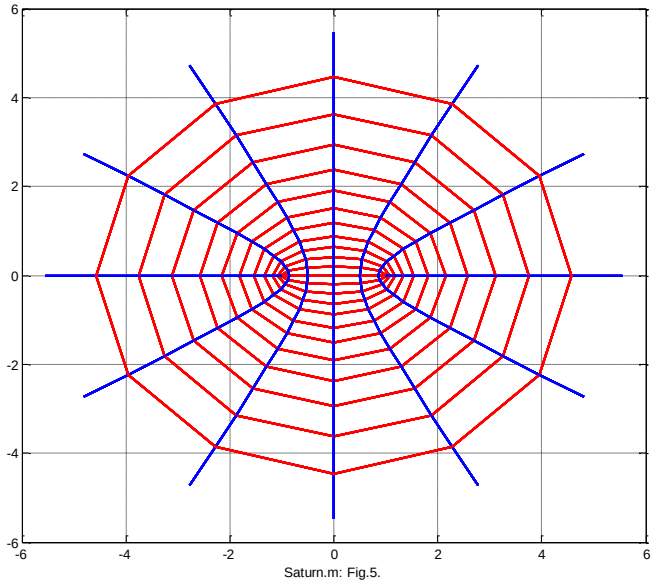

$$H_{\xi}. = h_{\xi}\Delta^{-2}\sin(\varphi)\cos(\varphi), \tag{8}$$

$$H_{\varphi}. = h_{\varphi}\Delta^{-2}\mathrm{sh}(\xi)\mathrm{ch}(\xi), \tag{9}$$

$$H_z = \Delta^{-2}, \tag{10}$$

$$J_{\xi} = \frac{2}{a\Delta^5}\sin(\varphi)\cos(\varphi), \tag{11}$$

$$J_{\varphi} = -\frac{2}{a\Delta^5}\mathrm{sh}(\xi)\mathrm{ch}(\xi), \tag{12}$$

$$J_z = \frac{3}{a\Delta^5}\left(h_{\varphi}\mathrm{sh}^2(\xi)\mathrm{ch}^2(\xi) - h_{\xi}\sin^2(\varphi)\cos^2(\varphi)\right), \tag{13}$$

where constants h_{ξ}, h_{φ} correlate through the following relation

$$h_{\xi} + h_{\varphi} = 0. \tag{14}$$

Diagrams of functions (8-13) under $a=1,\ h_{\xi}=1,\ h_{\varphi}=-1$ are shown in Fig. 6 on planes $(x,\ y)$, where $(x,\ y)$ are defined according to. Diagrams of functions (8-13) under $a=1,\ h_{\xi}=1,\ h_{\varphi}=-1$ are shown on Fig. 6 on planes $(x,\ y)$, where $(x,\ y)$ are defined according to function (7c) in relation to $0 \le \xi < \xi_{\max},\ 0 \le \varphi < 2\pi$.

The left column in Fig. 7 states functions $H_{\xi}(\xi)$, $H_{\varphi}(\xi)$, $H_z(\xi)$ under the stated value of φ. Furthermore, a solid line, dots and a dashed

line show these functions under $\varphi = 1.05,\ 1.83,\ 3.67$ respectively.

The right column in Fig. 7 states functions $H_\xi(\varphi),\ H_\varphi(\varphi),\ H_z(\varphi)$ under the stated value of ξ. Furthermore, a solid line, dots and a dashed line show these functions under $\xi = 0.4,\ 0.7,\ 1.4$ respectively.

Finally, Fig. 8 states functions $J_\xi(\xi),\ J_\varphi(\xi),\ J_z(\xi)$ and $J_\xi(\varphi),\ J_\varphi(\varphi),\ J_z(\varphi)$ in the same way.

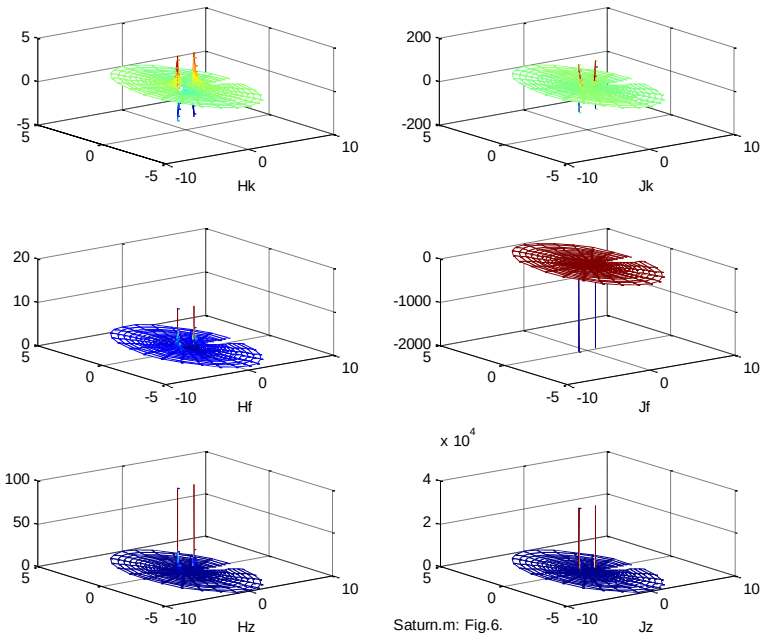

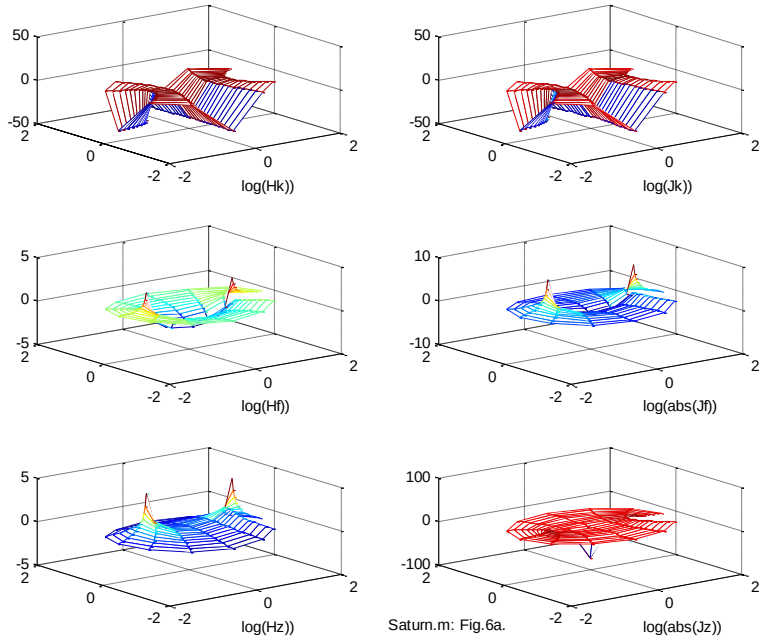

Saturn.m: Fig.6a.

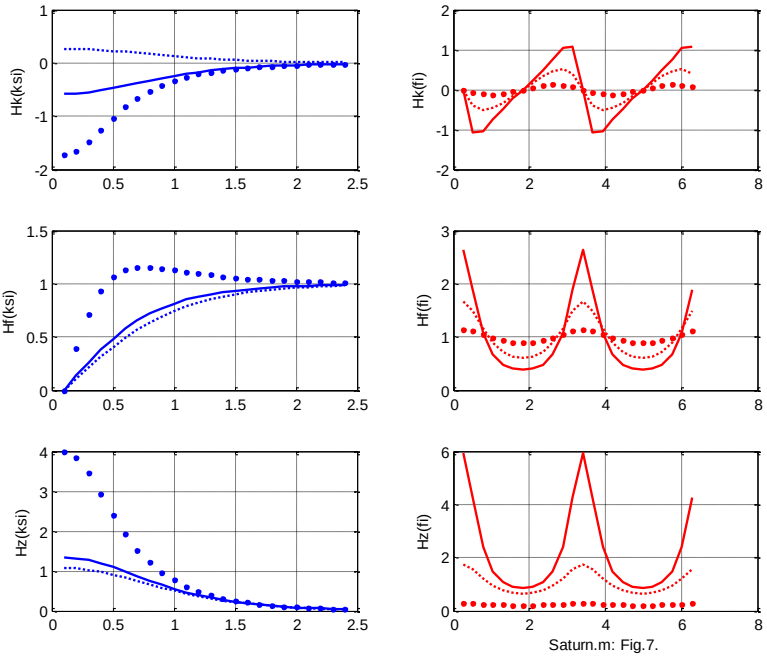

Saturn.m: Fig.7.

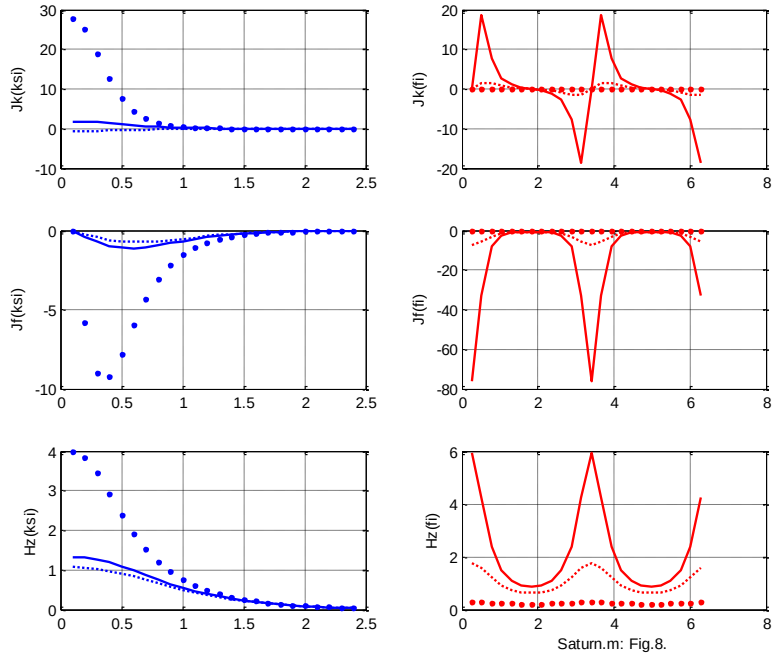

Saturn.m: Fig.8.

4. Mathematical model of hexagonal vortex

The image shown in Fig. 4 is determined by the initial conditions – – massive currents in the bottom of the vortex. In case of several sets of independent initial conditions, several solutions in the specified form occur. As the system of Maxwell's equations is linear, then actual solution is a sum of these several solutions. If the group of initial conditions determines a group of elliptic vortices with a common center, then the common solution will determine the vortex, shaping total ellipses.

It can be shown that the shape of total ellipses represents a closed curve Γ. This means that the locus of points with constant vertical vector of pressure on a free surface differs from a circle of the stated radius having a form of a closed curve Γ. The value of the vertical vector of pressure on this curve Γ will be of the same value. Consequently, in this case the surface of the vortex would be concentric curves Γ instead of concentric circles.

Each closed convex curve Γ can be decomposed into a sum of ellipses. Evidence may be as follows. Any such curve can be represented with two functions of angle φ:

$$x = f_x(\varphi), \quad (1)$$

$$y = f_y(\varphi). \quad (2)$$

Discrete functions (1, 2) represented in this way can be decomposed into trigonometrical series of the following kind:

$$x = \sum_{n=2}^{N} x_n , \tag{3}$$

$$y = \sum_{n=2}^{N} y_n , \tag{4}$$

where

$$x_n = \left(\alpha_n \cos\left(\frac{2\pi(n-1)}{N} \varphi \right) + \beta_n \sin\left(\frac{2\pi(n-1)}{N} \varphi \right) \right), \tag{5}$$

$$y_n = \left(\eta_n \cos\left(\frac{2\pi(n-1)}{N} \varphi \right) + \lambda_n \sin\left(\frac{2\pi(n-1)}{N} \varphi \right) \right). \tag{6}$$

Here, each pair of summands $(x_n,\ y_n)$ is an ellipse. Consequently, the curve Γ is a sum of ellipses.

Appendix 2 describes expansion of the hexagon into ellipses. The solution for elliptic vortex is stated above. Consequently, there is a possible group of initial conditions for a hexagonal vortex. Observations of Saturn and the Bermuda triangle proved existence of the above-mentioned combination of initial conditions.

Appendix 1. Solution of Maxwell's equations in cylindrical coordinates

Section 3 describes Maxwell's equations in elliptic coordinates $\xi,\ \varphi,\ z$ (3.4- 3.7a).

Let's find the solution of these equations assuming that all variables are unchanged along axis **z**. In this case, equations (2, 11-13, 14) will be as follows:

$$\frac{1}{\Delta^2}\left(\mathrm{sh}(\xi)\mathrm{ch}(\xi)H_\xi + \sin(\varphi)\cos(\varphi)H_\varphi\right) + \left(\frac{\partial H_\xi}{\partial \xi} + \frac{\partial H_\varphi}{\partial \varphi} \right) = 0, \tag{1}$$

$$\frac{1}{a\Delta} \frac{\partial H_z}{\partial \varphi} = J_\xi , \tag{2}$$

$$-\frac{1}{a\Delta} \frac{\partial H_z}{\partial \xi} = J_\varphi , \tag{3}$$

$$\left(\frac{1}{a\Delta^3}\left(\mathrm{ch}(\xi)\mathrm{sh}(\xi)H_\varphi - \cos(\varphi)\sin(\varphi)H_\xi\right) + \frac{1}{a\Delta}\left(\frac{\partial H_\varphi}{\partial \xi} - \frac{\partial H_\xi}{\partial \varphi} \right) \right) = J_z , \tag{4}$$

$$\frac{1}{\Delta^2}\left(\mathrm{sh}(\xi)\mathrm{ch}(\xi)J_\xi+\sin(\varphi)\cos(\varphi)J_\varphi\right)+\left(\frac{\partial J_\xi}{\partial\xi}+\frac{\partial J_\varphi}{\partial\varphi}\right)=0. \quad (5)$$

From (3.7b) we find that

$$\frac{\partial\left(\Delta^{-2}\right)}{\partial\xi}=\frac{\partial\left(\left(\mathrm{ch}^2(\xi)-\cos^2(\varphi)\right)^{-1}\right)}{\partial\xi}=2\Delta^{-4}\mathrm{sh}(\xi)\mathrm{ch}(\xi), \quad (6)$$

$$\frac{\partial\left(\Delta^{-2}\right)}{\partial\varphi}=\frac{\partial\left(\left(\mathrm{ch}^2(\xi)-\cos^2(\varphi)\right)^{-1}\right)}{\partial\xi}=2\Delta^{-4}\sin(\varphi)\cos(\varphi). \quad (7)$$

Let

$$H_\xi.=h_\xi\Delta^{-2}\sin(\varphi)\cos(\varphi), \quad (8)$$

$$H_\varphi.=h_\varphi\Delta^{-2}\mathrm{sh}(\xi)\mathrm{ch}(\xi). \quad (9)$$

Then

$$\frac{\partial H_\xi}{\partial\xi}=h_\xi\sin(\varphi)\cos(\varphi)\frac{\partial\left(\Delta^{-2}\right)}{\partial\xi}=2\Delta^{-4}h_\xi\sin(\varphi)\cos(\varphi)\mathrm{sh}(\xi)\mathrm{ch}(\xi), \quad (10)$$

$$\frac{\partial H_\xi}{\partial\varphi}=h_\xi\sin(\varphi)\cos(\varphi)\frac{\partial\left(\Delta^{-2}\right)}{\partial\varphi}=2\Delta^{-4}h_\xi\sin^2(\varphi)\cos^2(\varphi), \quad (11)$$

$$\frac{\partial H_\varphi}{\partial\varphi}=h_\varphi\mathrm{sh}(\xi)\mathrm{ch}(\xi)\frac{\partial\left(\Delta-^2\right)}{\partial\varphi}=2h_\varphi\Delta^{-4}\mathrm{sh}(\xi)\mathrm{ch}(\xi)\sin(\varphi)\cos(\varphi), \quad (12)$$

$$\frac{\partial H_\varphi}{\partial\xi}=h_\varphi\mathrm{sh}(\xi)\mathrm{ch}(\xi)\frac{\partial\left(\Delta^{-2}\right)}{\partial\xi}=2\Delta^{-4}h_\varphi\mathrm{sh}^2(\xi)\mathrm{ch}^2(\xi). \quad (13)$$

From (1, 8-13) we find that

$$\frac{1}{\Delta^2}\begin{pmatrix}\mathrm{sh}(\xi)\mathrm{ch}(\xi)h_\xi\Delta^{-2}\sin(\varphi)\cos(\varphi)+\\ \sin(\varphi)\cos(\varphi)h_\varphi\Delta^{-2}\mathrm{sh}(\xi)\mathrm{ch}(\xi)\end{pmatrix}+\begin{pmatrix}2\Delta^{-4}h_\xi\sin(\varphi)\cos(\varphi)\mathrm{sh}(\xi)\mathrm{ch}(\xi)+\\ 2\Delta^{-4}h_\varphi\mathrm{sh}(\xi)\mathrm{ch}(\xi)\sin(\varphi)\cos(\varphi)\end{pmatrix}=0$$

or

$$3h_\xi\sin(\varphi)\cos(\varphi)\mathrm{sh}(\xi)\mathrm{ch}(\xi)+3h_\varphi\mathrm{sh}(\xi)\mathrm{ch}(\xi)\sin(\varphi)\cos(\varphi)=0$$

or

$$h_\xi+h_\varphi=0. \quad (14)$$

From (4, 8-13) we find that

$$\begin{pmatrix}\frac{1}{a\Delta^3}\left(\mathrm{ch}(\xi)\mathrm{sh}(\xi)h_\varphi\Delta^{-2}\mathrm{sh}(\xi)\mathrm{ch}(\xi)-\cos(\varphi)\sin(\varphi)h_\xi\Delta^{-2}\sin(\varphi)\cos(\varphi)\right)+\\ \frac{1}{a\Delta}\left(2\Delta^{-4}h_\varphi\mathrm{sh}^2(\xi)\mathrm{ch}^2(\xi)-2\Delta^{-4}h_\xi\sin^2(\varphi)\cos^2(\varphi)\right)\end{pmatrix}=J_z$$

or

$$\left(\begin{array}{l}\left(h_\varphi \mathrm{ch}(\xi)\mathrm{sh}(\xi)\mathrm{sh}(\xi)\mathrm{ch}(\xi) - h_\xi \cos(\varphi)\sin(\varphi)\sin(\varphi)\cos(\varphi)\right)+ \\ \left(2h_\varphi \mathrm{sh}^2(\xi)\mathrm{ch}^2(\xi) - 2h_\xi \sin^2(\varphi)\cos^2(\varphi)\right)\end{array}\right) = a\Delta^{-5} J_z$$

or

$$3h_\varphi \mathrm{sh}^2(\xi)\mathrm{ch}^2(\xi) - 3h_\xi \sin^2(\varphi)\cos^2(\varphi) = a\Delta^{-5} J_z$$

or

$$J_z = \frac{3}{a\Delta^5}\left(h_\varphi \mathrm{sh}^2(\xi)\mathrm{ch}^2(\xi) - h_\xi \sin^2(\varphi)\cos^2(\varphi)\right) \tag{15}$$

By substitution of (2, 3) into (4), we will obtain the following

$$\frac{1}{\Delta^2}\left(\mathrm{sh}(\xi)\mathrm{ch}(\xi)\frac{1}{a\Delta}\frac{\partial H_z}{\partial \varphi} - \sin(\varphi)\cos(\varphi)\frac{1}{a\Delta}\frac{\partial H_z}{\partial \xi}\right)+$$

$$+\left(\frac{1}{a\Delta}\frac{\partial^2 H_z}{\partial \varphi \partial \xi} - \frac{1}{a\Delta}\frac{\partial^2 H_z}{\partial \varphi \partial \xi}\right) = 0$$

or

$$\left(\mathrm{sh}(\xi)\mathrm{ch}(\xi)\frac{\partial H_z}{\partial \varphi} - \sin(\varphi)\cos(\varphi)\frac{\partial H_z}{\partial \xi}\right) = 0. \tag{16}$$

From (6, 7) we find that

$$\left(\mathrm{sh}(\xi)\mathrm{ch}(\xi)\frac{\partial\left(\Delta^{-2}\right)}{\partial \varphi} - \sin(\varphi)\cos(\varphi)\frac{\partial\left(\Delta^{-2}\right)}{\partial \xi}\right) = 0. \tag{17}$$

Comparing (16, 17), we can notice that

$$H_z = \Delta^{-2}. \tag{18}$$

From (2, 3, 18), we obtain:

$$J_\xi = \frac{1}{a\Delta}\frac{\partial\left(\Delta^{-2}\right)}{\partial \varphi}, \tag{19}$$

$$J_\varphi = -\frac{1}{a\Delta}\frac{\partial\left(\Delta^{-2}\right)}{\partial \xi}. \tag{20}$$

or, taking (6, 7) into account,

$$J_\xi = \frac{2}{a\Delta^5}\sin(\varphi)\cos(\varphi), \tag{21}$$

$$J_\varphi = -\frac{2}{a\Delta^5}\mathrm{sh}(\xi)\mathrm{ch}(\xi). \tag{22}$$

Thus, if variables H_ξ. and H_φ are determined according to (8, 9), respectively, then variables H_z, J_ξ, J_φ, J_z are determined according to (18, 21, 22, 15), respectively, and condition (14) is satisfied.

Appendix 2. Decomposition of hexagon into ellipses.

Let's consider a hexagon shown in Fig. 1. It can be represented by two functions of angle φ:

$$x = f_x(\varphi), \quad (1)$$

$$y = f_y(\varphi). \quad (2)$$

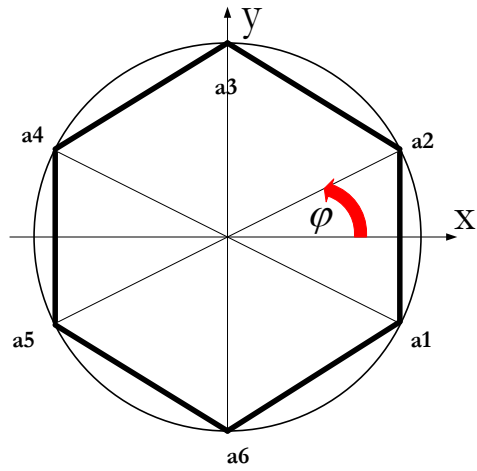

Fig. 1.

These functions are shown in Fig. 2. Let's represent these functions as a set of points. In Fig. 2 each line section is represented by three points: $n = 3$, and line section [a1, a2] is duplicated. In this case each function is described by $N = 7n$ points. Discrete functions (1, 2) determined in such a way can be decomposed into the trigonometric series of the form (4.1, 4.2).

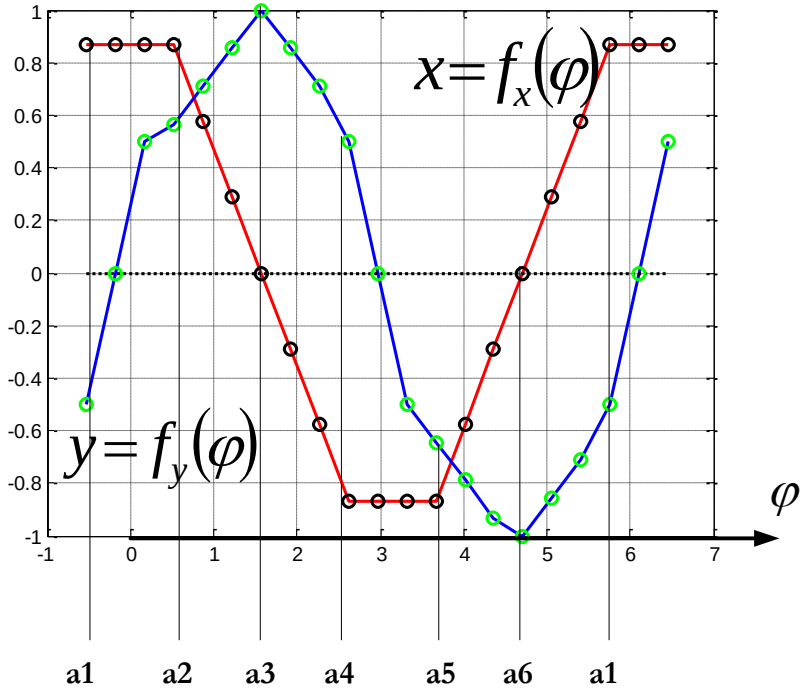

Рис. 2.

Modeling showed that for $n=1$ the constant values of first components can be neglected. Therefore, functions (1, 2) in polar and cylindrical coordinates can be approximated by $(N-1)$ functions, which describe **ellipses.** The sum of these functions represents a hexagon. For example, Fig. 3 and Fig. 4 show geometric objects obtained as a result of such approximation for $n=3$ and $n=9$, respectively. Fig. 6 shows the first 4 ellipses in the decomposition of the hexagon for $n=3$. The first ellipse is shown in dots.

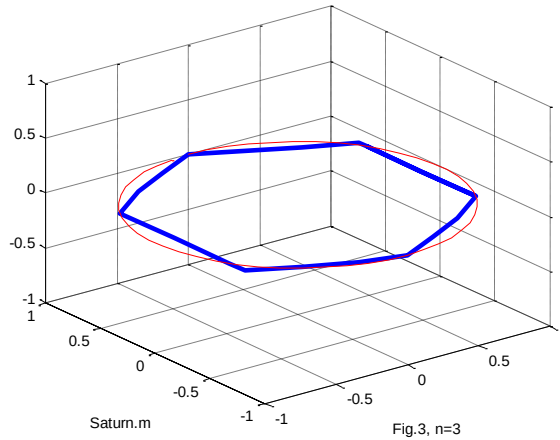

Saturn.m Fig.3, n=3

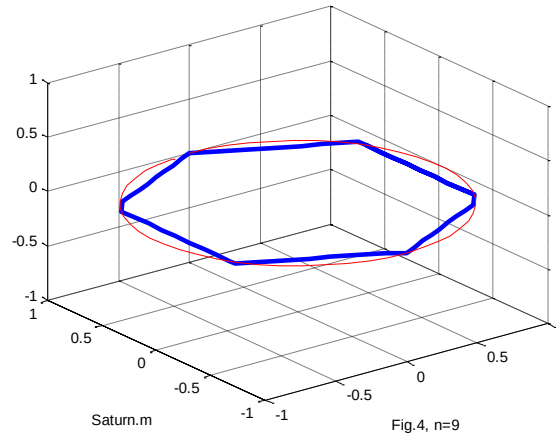

Saturn.m Fig.4, n=9

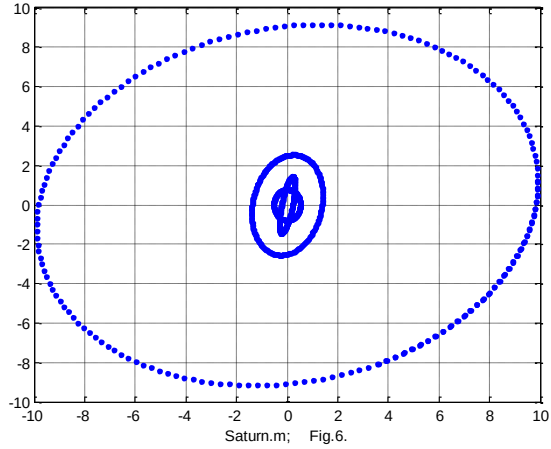

Saturn.m; Fig.6.

References

1. Saturn's hexagon, http://naucaitechnika.ru/blog/43524663032/10-strannyih-obektov-Solnechnoy-sistemyi,-o-kotoryih-nam-malo-ch (in Russian)
2. Saturn's hexagon, http://fishki.net/1592643-krupnye-inoplanetnye-buri-i-uragany.html (in Russian)
3. Saturn's hexagon, https://en.wikipedia.org/wiki/Saturn%27s_hexagon
4. It disclosed the secret of the Bermuda Triangle, https://lenta.ru/news/2016/10/24/bt/ (in Russian)
5. Khmelnik S.I. The Equation of Whirlpool, http://vixra.org/abs/1506.0157.
6. Khmelnik S.I. Experimental Clarification of Maxwell-Similar Gravitation Equations, http://vixra.org/abs/1311.0023; and «The Papers of Independent Authors», publ. «DNA», printed in USA, ISSN 2225-6717, Lulu Inc., ID 14794393, 2014, №28, ISBN 978-1-312-23676-9, http://lib.izdatelstwo.com/Papers/28.104.pdf
7. Andre Ango. Mathematics for Electrical and Radio Engineers, publ. "Nauka", Moscow, 1964, 772 p. (in Russian).
8. S.I. Khmelnik. Hexagonal Storm on Saturn, http://vixra.org/abs/1611.0313, 2016-11-23